The advantages of methanol-amine solvent mixtures in solution processing of Ge-Sb-S chalcogenide glass thin films

Jiri Jancalek ¹, Stanislav Slang ^{1,*}, Jiri Jemelka ², Peyton D. Simpson ³, Michal Kurka ¹, Jakub Houdek ¹, Karel Palka ^{1,2}, Miroslav Vlcek ^{1,2}

Abstract

We report on the substantial influence of methanol presence on the dissolution mechanism of $Ge_{20}Sb_5S_{75}$ bulk glass with subsequent superior properties of thin films deposited from such solutions. Raman spectroscopy confirmed significant differences in structural features present in glass solutions prepared from pure amines (n-propylamine and n-butylamine) and their mixtures with methanol. The experiments with dissolved elemental sulfur and $Ge_{25}S_{75}$ glass analog proved that both antimony and methanol presence induce further splitting of the $Ge_4S_{10}{}^4$ cluster structure, which fundamentally affects the properties of deposited thin films. Significant structural and compositional differences were found not only in solutions and as-prepared samples, but also after thin films' thermal treatment (hard baking up to 210°C). The as-prepared thin films deposited from amine-methanol mixtures possessed the exact composition of source bulk glass while thin films of other solvent formulations exhibited sulfur deficiency. The annealing up to 210°C only highlighted this difference. As a result of the different structure of the thin films prepared in this way, the other benefits of methanol addition were found, namely an increase in the refractive index by approx. 0.1 independent of the annealing temperature, or a lower thermally induced thickness contraction (up to 7.5%).

Keywords

Thin films, Sol-gel processes, Amorphous materials, Optical materials

Introduction

Amorphous and crystalline chalcogenide materials are used in a wide variety of advanced applications such as infrared optics [1-2], thermoelectric devices [3-4], solid-state electrolytes and/or electrodes for next-generation batteries [5-6] or phase change memories for neuromorphic computing [7]. In many of these applications, a thin film form is required. Currently, physical vapor deposition techniques (e.g., thermal evaporation [8-9], sputtering [10-11], pulse laser deposition [11], chemical vapor deposition [12]) are usually used for thin film deposition. These methods can prepare high-quality thin films at the cost of a large amount of energy input, a high vacuum environment, and high investment costs of processing equipment.

Solution-based deposition route provides a low-cost alternative for chalcogenide glass thin film deposition. By optimizing the solution deposition parameters, it is possible to achieve thin films of comparable quality using low-cost coating techniques (such as spin-coating [13 - 14], electrospray [15 - 14]).

¹ Center of Materials and Nanotechnologies, Faculty of Chemical Technology, University of Pardubice, Studentska 95, Pardubice 532 10, Czech Republic

² Department of General and Inorganic Chemistry, Faculty of Chemical Technology, University of Pardubice, Studentska 95, Pardubice 532 10, Czech Republic

³ Department of Chemistry, Austin Peay State University, 601 College St., Clarksville, TN, 37044, USA

^{*} stanislav.slang@upce.cz

- 16], inkjet printing [17 - 18] or chemical bath deposition [19 -20]). The advantage of the solution processing approach lies in the possibility of composite optical materials fabrication (e.g. doping with luminescent nanoparticles or other nanomaterials), which would not be possible by conventional physical vapor deposition techniques [21 - 22]). Especially Ge-S and Ge-Sb-S-based thin films proved to be suitable host media for doping applications [21, 23 - 24]. Recently, spin-coated thin films were used as suitable materials for the production of diffractive optical elements using electron beam and optical lithography [25], and hot-embossing techniques [26 - 27]. Notably, the $Ge_{20}Sb_5S_{75}$ solution-processed thin films could simultaneously serve as grayscale resists for electron beam lithography (EBL) and UV lithography [28].

Since the 1980s, the solution processing techniques have been extensively studied for arsenicbased glasses [29]. Recently, the research focus is shifting to the solution processing of glasses based on germanium chalcogenides, but it is still limited to only a few representatives of compositions with overstoichiometry of chalcogen ($Ge_{25}S_{75}$ [30], $Ge_{23}Sb_7S_{70}$ [16, 31 – 34], $Ge_{20}Sb_5S_{75}$ [28], $Ge_{25-x}Se_{75+x}$ (X = 0, 5, 10) [35]) and stoichiometric GeSe₂ [36]. Pure n-propylamine or n-butylamine solvents are used almost exclusively for the dissolution and deposition of germanium-sulfur based thin films [30 -37]. According to previous studies, the dissolution mechanism of germanium-based glasses in pure anhydrous amines leads to the fragmentation of the original polymerized glass structure into (Ge₄S₁₀)⁻⁴ molecular clusters [38], known for their high susceptibility to pore formation [38 – 42]. The structure of the thin films prepared in this way remains very similar to the structure of the source solution [38]. In addition, elemental sulfur is released from the structure of the thin film, which results in its evaporation during annealing or exposure [28,30, 38]. Based on previous work with Ge_{20-x}Se_{75+x} thin films [35], it was confirmed that germanium-based glasses could be successfully deposited in specular optical quality from a mixture of pure amine with methanol, and subsequent annealing can easily minimize the content of organic residuals (including added methanol). However, this finding raises new questions about the applicability of methanol addition in preparation of previously studied Ge-S and Ge-Sb-S-based systems and how the presence of methanol influences the properties of Ge-based solution-processed thin films.

In this work, we present the study of methanol addition influence on the dissolution mechanism of $Ge_{20}Sb_5S_{75}$ source bulk glass and subsequently on the structure of spin-coated thin films. The aim of the research is to explain the role of amine solvent mixtures and the presence of methanol on the formation of various glass structural units and the considerably positive impact of methanol addition on the physico-chemical properties of deposited thin films. The non-toxic $Ge_{20}Sb_5S_{75}$ composition was chosen to represent previously published works based on the Ge-Sb-S system [37, 43] with good chemical stability and high potential in practical applications. Based on our findings, the methanol addition not only significantly influence the Ge-Sb-S dissolution mechanism, but it is also highly beneficial for compositional stability, porosity, and refractive index of prepared thin films. Thus, the multi-component amine-methanol solvent approach is highly advantageous comparatively with previously published usage of pure amines.

Experimental

Materials

Germanium (Ge, 99.999 %, Alfa Aesar), antimony (Sb, 99.999%, Alfa Aesar) and sulfur (S, 99,999%, Alfa Aesar), n-propylamine (PA, purum, ≥99 %, Sigma-Aldrich), n-butylamine (BA, 99.5 %,

Sigma-Aldrich), methanol (MetOH, p.a., 99,5 %, Lach-Ner), nitric acid (HNO₃, p.a., 65 %, Lach-Net) and hydrochloric acid (HCl, p.a., 35 %, Penta) were used without further purification.

Bulk glass synthesis and thin film deposition

The source $Ge_{20}Sb_5S_{75}$ as well as $Ge_{25}S_{75}$ bulk glass were synthesized by a standard melt quenching method using high-purity (5N) elemental powders. Quartz ampules were cleaned using aqua regia to remove organic and inorganic impurities, then rinsed with deionized water, and dried. Appropriate quantities of pure elements were weighted into cleaned quartz ampule. Subsequently, the ampule was evacuated to a residual pressure of ~ 10^{-3} Pa and sealed. The synthesis was performed in a rocking tube furnace at 950°C for 72 hours. The quartz ampule with melted glass was quenched in cold water.

The prepared $Ge_{20}Sb_5S_{75}$ bulk glass was powdered in an agate bowl and dissolved in PA, BA, mixture of 10 vol% of MetOH in PA (PA-MetOH) and a mixture of 10 vol% of MetOH in BA (BA-MetOH) with a concentration of 0.075 g of glass powder per 1 ml of solvent (or solvent mixture). The synthetized $Ge_{25}S_{75}$ bulk glass was dissolved in PA and mixture of 10 vol% of MetOH in PA (PA-MetOH) also with a concentration of 0.075 g of glass powder per 1 ml of solvent. The next set of solutions was prepared by dissolving 0.0833 g of glass powder per 1 ml of amines (PA and BA) to determine the influence of methanol addition. After the complete glass dissolution, the pure methanol was subsequently added to reach the same glass concentration as in the previously prepared solutions (0.075 g of $Ge_{20}Sb_5S_{75}$ glass powder per 1 ml of solvent). The elemental sulfur in concentrations a) equivalent to glass sulfur overstoichiometry in $Ge_{20}Sb_5S_{75}$ glass (c = 0.015 g of sulfur per 1 ml of solvent) and b) all sulfur present in weighted glass (c = 0.04 g of sulfur in 1 ml of solvent) was also dissolved in both pure amines and amine-methanol mixtures. Dissolutions of bulk glasses and elemental sulfur were performed in nitrogen-filled glovebox LabMaster Pro_MB200 (MBraun) inside closed glass vials and under rigorous stirring (300 rpm) using multistirrer digital 6 (Velp). All prepared solutions were clear without any precipitate or turbidity.

The prepared chalcogenide glass solutions were used for the deposition of thin films by a spin-coating method using a WS-650Mz-23NPPB (Laurell) device. The deposition was performed in nitrogen-filled glovebox using 60 s spin-time and spin-rate of 4400 RPM for PA solutions, 2000 RPM for BA solutions, 4000 RPM for PA-MetOH solutions, and 2200 RPM for BA-MetOH solutions. Deposition parameters were chosen based on data from preliminary experiments with a target to obtain approx. 200 nm thickness of thin films annealed at 210°C (the highest annealing temperature). Freshly deposited thin films were immediately annealed at 60 °C on a hot plate HP 20D (Witeg) for 20 min, in inert nitrogen atmosphere (hereafter referred to as "as-prepared" thin films). The as-prepared thin films were subsequently thermally stabilized by annealing at temperatures 90, 120, 150, 180, and 210 °C for 1 hour in a nitrogen atmosphere. The entire process of solutions preparing, thin film deposition and their subsequent post-deposition annealing are shown in the diagram in supplementary information S1.

Characterization

The transmission spectra of studied thin films were measured using UV-VIS-NIR spectrometer UV3600 (Shimadzu) in the spectral range 190-2000 nm. The thicknesses and refractive index values of $Ge_{20}Sb_5S_{75}$ thin films were evaluated using the procedure described in [25]. Transparent region of thin films' transmission spectra (extinction coefficient $k \rightarrow 0$) was fitted by a model of transmission

spectrum presented by Swanepoel [44] (absorption in the thin films is neglected -i.e. k = 0), where the spectral dependence of the refractive index was expressed using the Wemple-DiDomenico's equation [45]:

$$n^2 - 1 = \frac{E_d E_0}{E_0^2 - (h\nu)^2} \tag{1},$$

where E_d is parameter of dispersion energy, E_0 is single oscillator energy and hv is photon energy. Described evaluation method is suitable for very thin films of dielectric materials when the measured transmission spectra exhibit insufficient number of interference fringes for classical Swanepoel's method to be used. The method's limitation is a necessary specular optical quality of analyzed thin films. An example of spectrum fitted by the described procedure in a transparent spectral region is depicted in Figure 1.

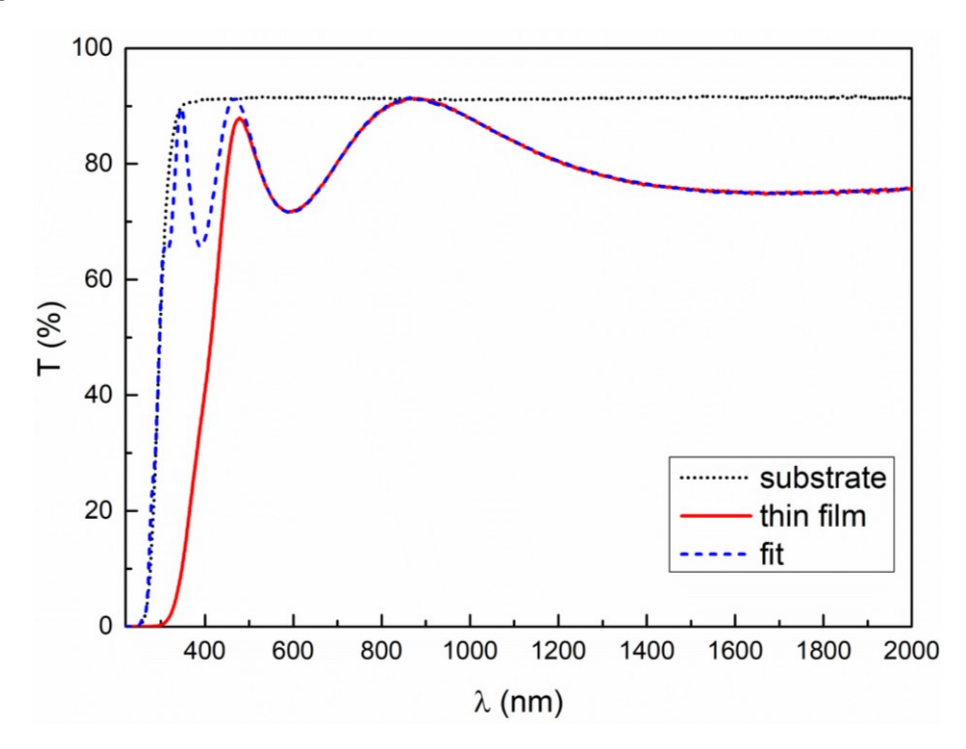


Figure 1: The example of the transmission spectrum of spin-coated $Ge_{20}Sb_5S_{75}$ thin film from butylamine-methanol mixture annealed at 210 °C (red solid line) and soda-lime glass substrate (black dotted line) together with fitted transmission spectrum (blue dashed line).

The presented thicknesses and refractive indexes represent average values obtained by measuring and evaluating of three samples of each treatment. Error bars represent the standard deviation of obtained values.

Thickness verification, topography, and surface roughness measurements of the thin films were performed using atomic force microscopy (AFM) in semi-contact mode using NTEGRA (NT-MDT) microscope equipped with NSG10 tips (AppNano). The thickness of the thin film was determined by measuring the depth of the scratch made by a steel needle through the thin film. Comparison of the determined thickness values obtained by the evaluation of the transmission spectrum and the thicknesses determined by AFM are shown in the table in the supplementary information S2. Stabilized thin films and thin films annealed at 210 °C were measured at 3 areas of 5 × 5 μ m. Sample AFM scans and the corresponding surface roughness of the thin films are shown in supplementary information S3.

The structure of source bulk glass, pure amines, amine-methanol mixtures, glass and elemental sulfur solutions as well as spin-coated chalcogenide glass thin films were studied by Raman spectroscopy using MultiRam (Bruker) FT-Raman spectrometer utilizing 1064 nm Nd:YAG laser excitation beam (2 cm⁻¹ resolution, averaging of 200 scans for liquid samples and 64 scans for solid samples). Raman spectra of solutions were normalized by the most intensive band of pure amines in the region of 100 - 500 cm⁻¹, and thin film spectra were normalized by the intensity of the band at 345 cm⁻¹ (edge shared tetrahedra of GeS_{4/2}).

The amorphous state of thin films was investigated by GI-XRD method using Empyrean diffractometer (Malvern Panalytical) fitted with non-ambient chamber DHS 1100 (Anton Paar). For the incident beam, copper anode (Cu K α = 1,54 Å), focusing mirror and 1/8° slits were used. The incidence angle was fixed at 1° to provide sufficient penetration depth (approx. 300 nm) for the whole thin film and minimize substrate background at the same time. 2Theta axis was scanned in the range of 10° to 70° with step size 0.0263° and counting time 500 s per step using PIXcel3D-Medipix3 1x1 detector. Samples were measured in a vacuum under carbon cover dome to avoid oxidation during measurement.

The scanning electron microscopy (FE-SEM) scans and elemental composition data were obtained using scanning electron microscope LYRA 3 (Tescan) equipped with EDS analyzer AZtec X-Max 20 (Oxford Instruments). The samples were analyzed by EDS on five 400 x 400 μ m areas at an accelerating voltage of 5 kV. The presented data show the average of measured values, and the error bars represent their standard deviation. The representative FE-SEM scans were obtained at an acceleration voltage of 10 kV, and they are presented in the supplementary part of this manuscript in Figure S4.

Results and discussions

The quantitative dissolution of $Ge_{20}Sb_5S_{75}$ in pure amines (both n-propylamine and n-butylamine) leads to clear, amber colored solutions (solution 1 on the Figure 2). On the contrary, the solutions prepared by dissolution of $Ge_{20}Sb_5S_{75}$ in a mixture of 90 vol.% of amines and 10 vol.% of methanol were significantly darker (solution 2 on the Figure 2) with a shade closer to the color of elemental sulfur dissolved both in pure amine and amine-methanol mixture (solution 3 on the Figure 2).



Figure 2: Photos of the prepared solutions: 1) $Ge_{20}Sb_5S_{75}$ from pure n-propylamine, 2) $Ge_{20}Sb_5S_{75}$ in the mixture of 90% n-propylamine and 10% of methanol, and 3) Sulfur dissolved in pure n-propylamine (c=0.04 g of sulfur/ml of the solution – corresponding with a total sulfur concentration in previous solution).

The substantial color difference between prepared Ge₂₀Sb₅S₇₅ solutions suggests that the presence of methanol instigates changes in the glass dissolution mechanism with a potential impact

on the properties of deposited solution-processed thin films. The structural features of prepared solutions were studied by Raman spectroscopy. Raman spectra of pure solvents, solvent mixtures and dissolved $Ge_{20}Sb_5S_{75}$ glass are presented in Figure 3. The spectra of pure n-propylamine and n-propylamine/methanol mixture in the studied $100-550~\text{cm}^{-1}$ region contained one distinctive band at 457 cm⁻¹, which was used to normalize the Raman spectra of all n-propylamine-containing solutions. Similarly, the intensive band at 400 cm⁻¹ was used to normalize the Raman spectra of all n-butylamine-containing solutions.

The Raman spectra of pure n-propylamine and n-butylamine $Ge_{20}Sb_5S_{75}$ solutions consist of well-developed bands at 141, 187, 338, 361, 377 and 472 cm⁻¹. The dominant bands at 141, 187, 338 and 472 cm⁻¹ indicate the presence of $Ge_4S_{10}^{4-}$ anions with a compensated negative charge by n-propylor n-butyl-ammonium cations [38]. The less intense band at 361 cm⁻¹ originates probably from dissolution products of antimony structures in the form of $Sb_4S_7^{2-}$ [46]. The origin of the low-intensity band at 377 cm⁻¹ is not entirely clear. Still, due its position and low intensity, we assume it could be a solution equivalent to the companion vibration of Ge-S-Ge structural units [47 – 51].

There is a significant difference between the spectra of $Ge_{20}Sb_5S_{75}$ solutions prepared from pure amines and amine methanol mixtures. Intensities of bands at 141, 187, 338, and 472 cm⁻¹ (dissolution products based on $Ge_4S_{10}^4$) are decreasing, whereas the intensity of the band at 361 cm⁻¹ is increasing ($Sb_4S_7^2$ based dissolution products). Since the increase in the intensity of the band at 361 cm⁻¹ is more pronounced than can be expected only from antimony structures, we assume that in addition to the antimony bands, bands of a new unknown Ge-S dissolution product may also contribute to the intensity of this band. Moreover, a new broad band around 420 cm⁻¹, which can be attributed to the terminal Ge-S⁻ stretching vibration [52], is present in the measured spectra. According to these observations, we can state that the presence of methanol during the dissolution of $Ge_{20}Sb_5S_{75}$ chalcogenide glass induces the splitting of the original glass structure to smaller $Ge-S^-$ structural units in comparison with the solution originating from pure amines.

To determine the alcohol role in glass dissolution, the methanol was also added into already prepared n-propylamine and n-butylamine $Ge_{20}Sb_5S_{75}$ glass solutions. The Raman spectra (Figure 3) showed that the solutions with subsequently added methanol are structurally more fragmented in comparison with solutions of glass dissolved in pure amines (simultaneous intensity decrease of bands at 141, 187, 338 and 472 cm⁻¹ and increase of bands at 361 and 420 cm⁻¹) but not to a level corresponding to the complete glass dissolution in the mixture of amine and methanol. It indicates that methanol is undoubtedly participating in $Ge_{20}Sb_5S_{75}$ glass dissolution, and partially influences post-dissolution equilibrium. Thus, the simple addition of methanol into the already prepared pure amine solution will not result in the similar glass structural fragmentation as in solution prepared directly from mixed solvent.

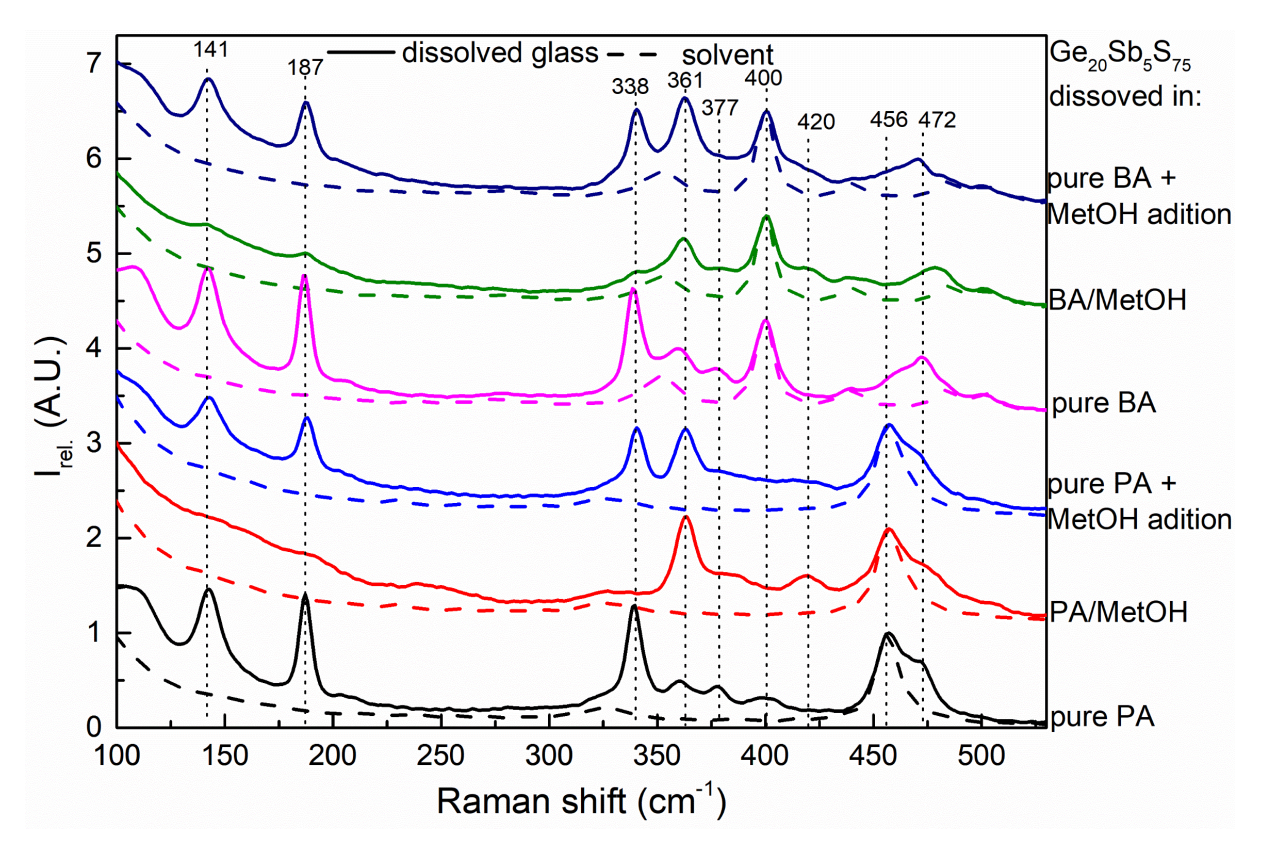


Figure 3: Raman spectra of $Ge_{20}Sb_5S_{75}$ chalcogenide glass dissolved in pure amine and amine-methanol mixture solvents.

The Raman spectra of prepared solutions also showed that methanol presence during dissolution has a significant impact on the intensity of the bands corresponding to the vibration of dissolution products of sulfur in amines (mainly S_3^- and S_4^{2-} polysulfides) [53 – 54]. In order to verify the effect of methanol presence on the sulfur dissolution mechanism, the set of elemental sulfur solutions with various concentrations (0.015 and 0.04 g/ml) and solvent formulations (pure npropylamine and n-propylamine-methanol mixture) were prepared (Figure 4). The chosen concentrations correspond either to sulfur overstoichiometry in the Ge₂₀Sb₅S₇₅ solutions or the total amount of sulfur in prepared solutions. The Raman spectra confirmed that the presence of methanol does not induce the formation of different sulfur dissolution products and therefore the observed structural changes are not related to overstoichiometric sulfur but take place based on different Ge-S and/or Sb-S dissolution structural units. To distinguish the influence of Sb-presence on Ge₂₀Sb₅S₁₅ glass solution, the Ge₂₅S₇₅ glass analogue was dissolved as well (Figure 4). Surprisingly, the results clearly show, that methanol presence during glass dissolution only partially decreases the intensities of Ge₄S₁₀⁴⁻ vibrations bands at 141, 187, 338 and 472 cm⁻¹ while the Ge-S⁻ stretching vibration band at 420 cm⁻¹ increases. Unlike in the case of Ge₂₀Sb₅S₇₅ glass, there is no increase in the band at 361 cm⁻¹ and only a partial decrease of the ${\rm Ge_4S_{10}}^4$ bands. Thus we assume that the presence of antimony is essential for the cleavage of the glass molecular structure to the level of Ge₂₀Sb₅S₇₅ solutions in the aminemethanol mixtures.

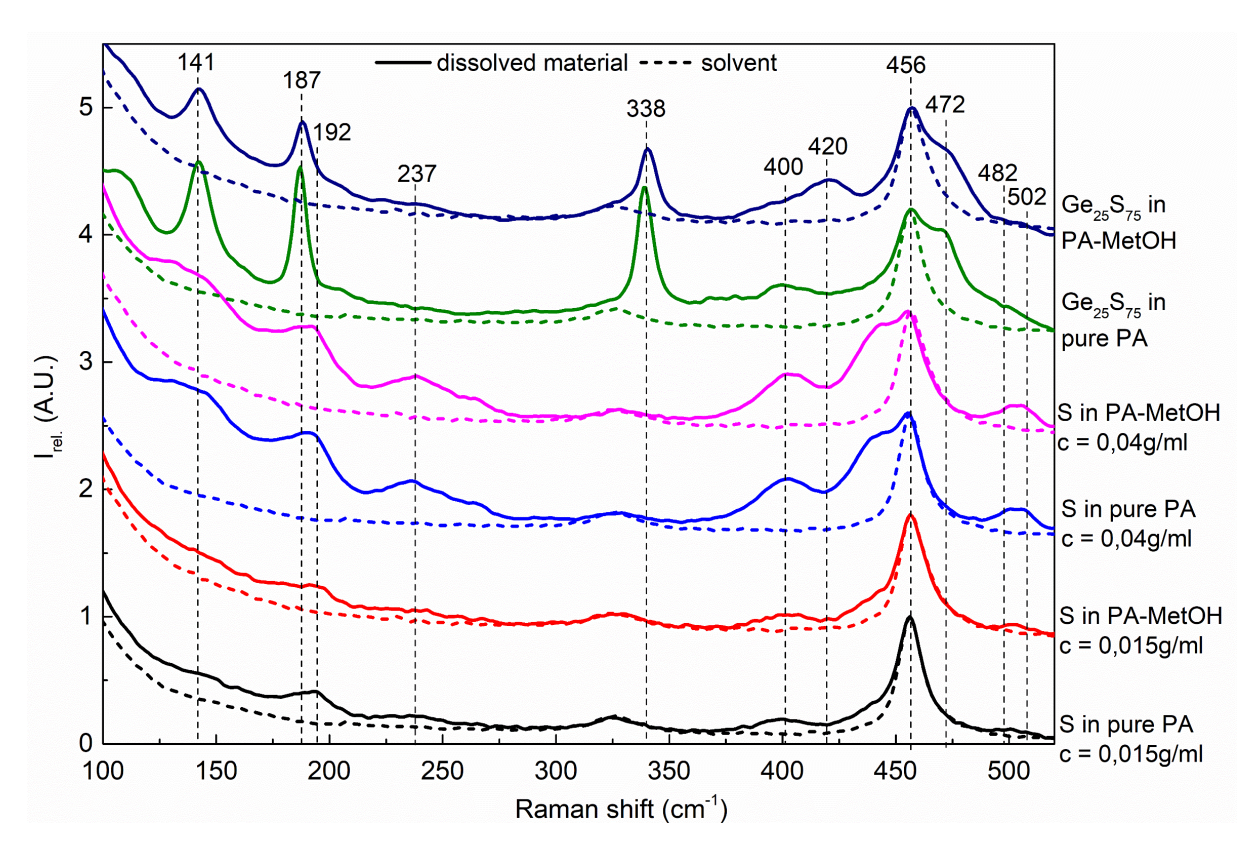


Figure 4: Raman spectra of sulfur dissolved at various concentrations and Ge₂₅S₇₅ chalcogenide glass in pure PA and PA-MetOH mixture.

Based on our findings, we conclude that methanol presence significantly alters the dissolution mechanism and established equilibrium in the final $Ge_{20}Sb_5S_{75}$ solution. Our observed results of the dissolution of $Ge_{20}Sb_5S_{75}$ glass in pure amine are consistent with the dissolution mechanism described in [38], i.e. the dissolution of $Ge_{20}Sb_5S_{75}$ glass structures in pure aliphatic amine leads to the formation of stable $[Ge_4S_{10}]^{4-}$ ions compensated by n-propylammonium or n-butylammonium cation. Similarly, the observed dissolution of Sb-S structures leads analogically to the formation of $Sb_4S_7^{2-}$ in solution. The presence of methanol leads to the fractionation of the $Ge_{20}Sb_5S_{75}$ structure to the molecular level $(Ge_4S_{10}^{4-}$ bands are absent), while the antimony structural units based on $Sb_4S_7^{2-}$ remain stable in studied solutions. Overstoichiometric sulfur, as well as part of sulfur from fractionated $Ge_{20}Sb_5S_{75}$ remains dissolved in the form of polysulfides (weak and wide bands of pure dissolved sulfur correspond to bands present in $Ge_{20}Sb_5S_{75}$ amine-methanol solutions). The methanol addition into already dissolved glass in pure amines only partially changes the structures of the final solution, which shows that methanol participates both in the dissolution process itself and in the stabilization of the final products. For this reason, the post-dissolution addition of methanol does not lead to the same ratio of dissolution products and only partially affects their final form.

The structure of source bulk glass and deposited thin films was also studied by Raman spectroscopy (Figure 5). The main Raman band of $Ge_{20}Sb_5S_{75}$ bulk glass belongs to the corner-shared tetrahedrons of $GeS_{4/2}$ and is located at 345 cm⁻¹ [55 – 57]. This band is asymmetrically broadened both to lower and higher Raman shifts, due to the presence of wide and low intensity band around 300 cm⁻¹ belonging to the vibrations of pyramidal units of $SbS_{3/2}$ [58], and the presence of bands at 368 and

 436 cm^{-1} corresponding with the to the vibrations in edge-shared tetrahedral units of $GeS_{4/2}$ [37, 55 – 58]. Sulfur overstoichiometry leads to the presence of ring S_8 bands at 151, 219, and 475 cm⁻¹ [30, 37].

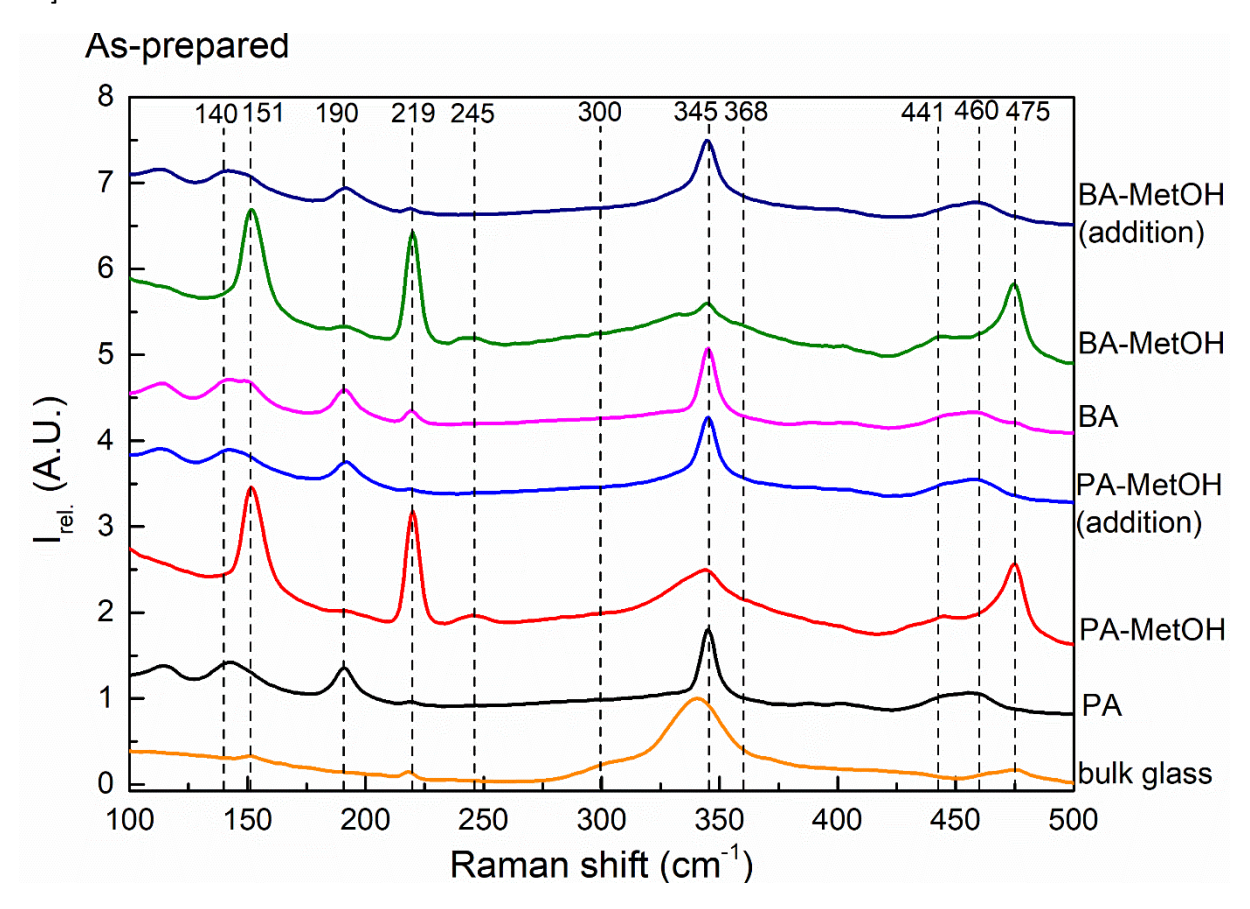


Figure 5: Raman spectra of as-prepared $Ge_{20}Sb_5S_{75}$ thin films from pure amines and mixtures of amine-methanol solution.

The Raman spectra of as-prepared $Ge_{20}Sb_5S_{75}$ thin films deposited from pure n-propylamine and n-butylamine solution significantly differ from the spectrum of source bulk glass. The main band at 344 cm⁻¹ is significantly narrower, which indicates the high fragmentation of the material's structure in the form of $GeS_{4/2}$ tetrahedra. The bands at 140, 190, and 460 cm⁻¹ confirm the presence of alkyl ammonium germanium sulfide (AAGS) salts [30, 37]. The fragmented structure of the as-prepared thin film indicates a strong similarity with structural fragments present in glass solution, as the bands in the solution and thin film share almost identical positions (141, 187, 338, and 472 cm⁻¹ bands, observed in solutions, are slightly shifted in thin films to 140, 190, 345 and 460 cm⁻¹).

Importantly, the methanol present in the source solution also significantly influences the Raman spectra of as-prepared thin films. In comparison to the pure amine-based thin films, the main band at 345 cm⁻¹ (corner-shared tetrahedrons $GeS_{4/2}$) is less intensive and noticeably broader. Similarly, to the Raman spectrum of bulk glass, the band at 345 cm⁻¹ is also asymmetrical due to the presence of bands around 300 cm⁻¹ (pyramidal units of $SbS_{3/2}$) and 368 cm⁻¹ (edge-shared tetrahedrons $GeS_{4/2}$). The bands corresponding to sulfur rings (151, 219, and 475 cm⁻¹) are significantly enhanced, while the intensity of bands corresponding to AAGS salts (140, 190, and 460 cm⁻¹) are suppressed. The new band can be found in spectra of amine-methanol mixture-based thin films at 245 cm⁻¹, which can be attributed to ethane-like $S_3Ge-GeS_3$ groups [50]. We assume, that the more complex structure of

thin films from amine-methanol mixture solutions is based on the rapid reaction of the highly fragmented glass structure of the solution and the transformation of polysulfide sulfur to the form of S_8 rings during the thin film formation process.

The Raman spectra of the thin film prepared from the solutions of dissolved glass in pure amines with the subsequent addition of methanol are almost the same as the Raman spectra of pure amine-based films. The main band at 345 cm $^{-1}$ is only slightly wider, given by the presence of edge shared tetrahedrons GeS $_{4/2}$.

With increasing annealing temperature, the Raman spectra of thin films become similar to the Raman spectrum of bulk glass (Figure 6). Therefore, in the case of pure amine-based thin films, the main band is getting broader, and the intensity of AAGS salts decreases due to the thermally induced AAGS decomposition and structural polymerization as reported in [30, 37]. In the case of thin films deposited from an amine-methanol mixture, the noticeable decrease in intensity of S₈ sulfur ring bands can be observed due to their gradual incorporation into Ge-S structures. Unfortunately, measurements of the thin films annealed at 210°C could not be performed due to the oversaturation of the Raman detector with a luminescence signal even at the lowest excitation laser power. However, the absence of sharp peaks in XRD spectrum (except for the peak at 29.34° belonging to the carbon dome) confirms the amorphous character of all studied thin films annealed event at the highest temperatures (Fig.7).

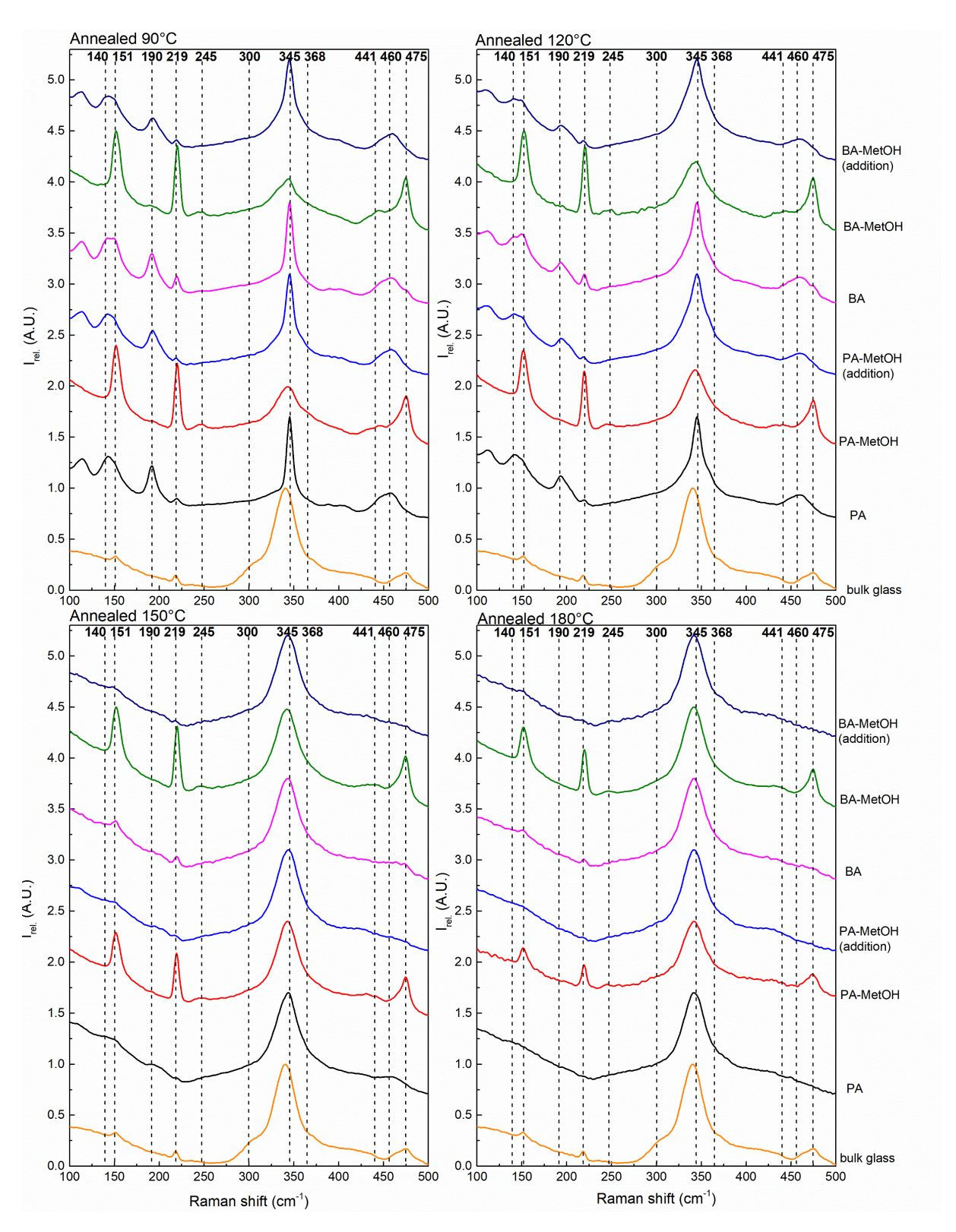


Figure 6: Raman spectra of $Ge_{20}Sb_5S_{75}$ thin films annealed at different temperatures in the range of 90 - 180°C prepared from solutions based on pure amines and amine-methanol mixtures.

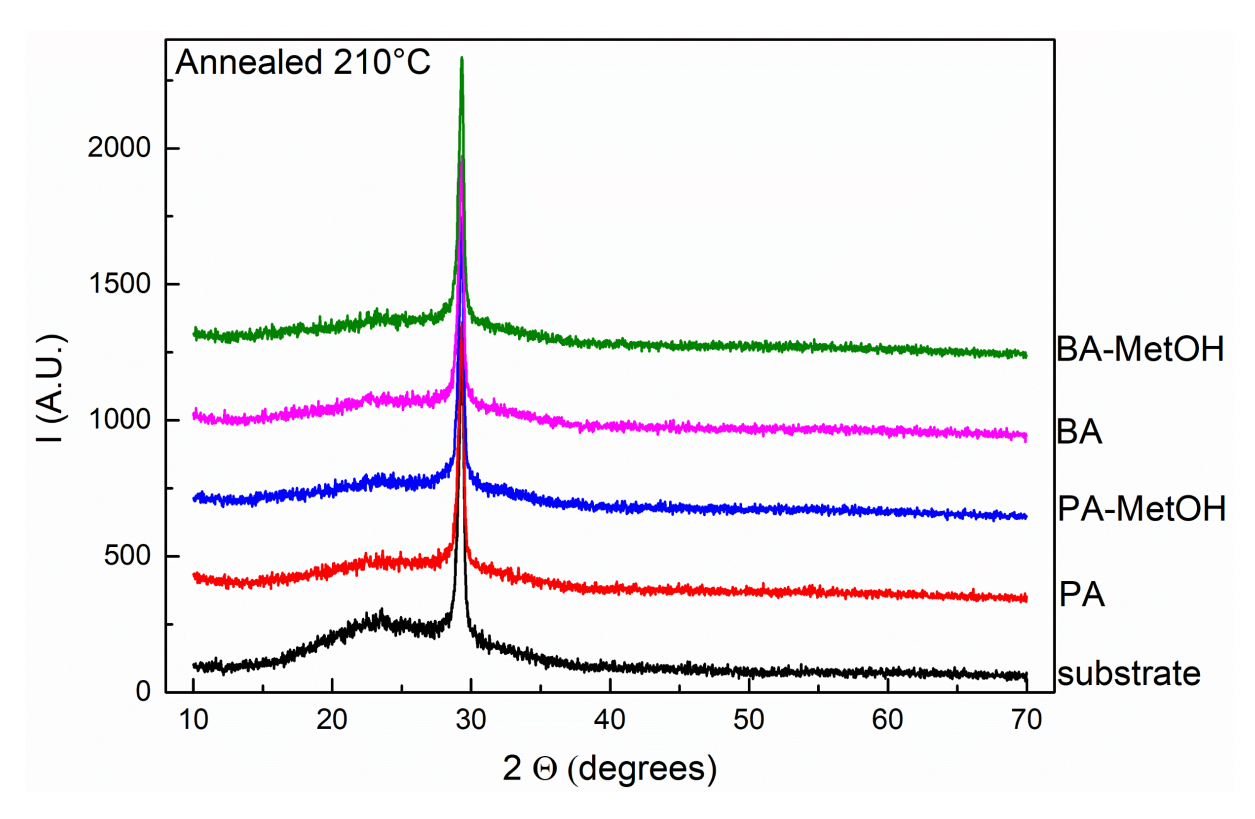


Figure 7: XRD patterns of the highest temperature annealed $Ge_{20}Sb_5S_{75}$ thin films deposited from pure amines and mixtures of amine-methanol solution.

The composition of the studied thin film was analyzed by EDS. Notably, the experimental data (Table 1 and Figure 8) shows a significant sulfur deficit in as-prepared thin films prepared both from pure amine solutions and solutions with methanol added after complete glass dissolution. Moreover, the sulfur content is also decreases with increasing annealing temperature (Figure 8). The total amount of missing sulfur reaches between 5-7 at. % (in comparison with the targeted Ge₂₀Sb₅S₇₅ composition). Contrary, the as-prepared thin films deposited from solutions of amine-methanol mixtures possess nearly ideal Ge₂₀Sb₅S₇₅ composition and thermal stabilization induces only a minor decline of sulfur content. This fact is crucial for further solution processing of other Ge-based chalcogenide glass thin films, as maintaining the targeted composition is necessary for further practical applications of such an approach. The missing sulfur in as-prepared thin films deposited from solution without methanol during glass dissolution can be potentially explained by significant structural and morphological differences of deposited thin films. We assume that co-evaporation of occluded amine residua with dissolved polysulfide reaction products (AAGS salts) together with nano-porosity of such prepared thin films [38-42] play a key role in observed sulfur depletion. During the deposition process, the $Ge_4S_{10}^{4-}$ ionic salts transform into the corner-shared tetrahedrons of GeS_{4/2}. The sulfur excess probably remains bound in the form of the alkyl ammonium salts. During post-deposition thermal stabilization, the salts decompose forming H₂S and other volatile products, which are released from the structure of Ge₂₀Sb₅S₇₅ thin films. This theory is in good agreement with observations in spin-coated As-S films [59 − 60]. It also explains the higher sulfur deficit of thin films deposited from the solution of more volatile n-propylamine in comparison to the slightly less volatile n-butylamine (vapor pressure at 20°C for n-propylamine is 339 hPa and for n-butylamine is 95.5 hPa) [61 – 62].

Table 1: Compositions of as-prepared and annealed $Ge_{20}Sb_5S_{75}$ thin films deposited from solutions of pure amines and mixtures of amine-methanol solvents.

PA	S	Ge	Sb	BA	S	Ge	Sb
60	72.4 ± 0.5	22.1 ± 0.1	5.5 ± 0.7	60	73.2 ± 0.7	21.7 ± 0.1	5.1 ± 0.7
90	71.5 ± 0.5	22.6 ± 0.1	5.9 ± 0.6	90	71.9 ± 0.5	22.0 ± 0.2	6.1 ± 0.4
120	70.3 ± 0.4	23.4 ± 0.1	6.3 ± 0.4	120	71.6 ± 0.4	22.8 ± 0.3	5.7 ± 0.5
150	69.6 ± 0.3	23.7 ± 0.1	6.7 ± 0.3	150	70.6 ± 0.3	23.0 ± 0.1	6.4 ± 0.4
180	69.4 ± 0.5	24.3 ± 0.1	6.3 ± 0.6	180	70.2 ± 0.6	23.5 ± 0.1	6.3 ± 0.7
210	67.8 ± 0.8	24.9 ± 0.1	7.3 ± 0.9	210	69.6 ± 0.6	24.6 ± 0.2	5.8 ± 0.7
PA - MetOH	S	Ge	Sb	BA - MetOH	S	Ge	Sb
60	74.2 ± 0.4	20.5 ± 0.2	5.2 ± 0.5	60	75.0 ± 0.5	20.1 ± 0.2	4.9 ± 0.6
90	74.2 ± 0.6	20.4 ± 0.1	5.4 ± 0.7	90	75.1 ± 0.4	20.2 ± 0.2	4.8 ± 0.4
120	74.2 ± 0.4	20.2 ± 0.1	5.6 ± 0.4	120	74.1 ± 0.6	20.3 ± 0.1	5.7 ± 0.6
150	74.1 ± 0.6	20.1 ± 0.1	5.8 ± 0.7	150	75.0 ± 0.4	21.9 ± 1.0	3.1 ± 1.4
180	74.0 ± 0.3	20.2 ± 0.1	5.8 ± 0.4	180	74.5 ± 0.3	20.2 ± 0.1	5.3 ± 0.4
210	73.9 ± 0.1	20.7 ± 0.2	5.5 ± 0.2	210	73.7 ± 0.2	20.6 ± 0.1	5.6 ± 0.2
PA -	c		ch	BA -	c	,	7
MetOH	S	Ge	Sb	MetOH	S	Ge	Sb
(addition)				(addition)			
60	71.6 ± 0.6	22.4 ± 0.2	5.9 ± 0.5	60	72.4 ± 0.7	22.2 ± 0.2	5.4 ± 0.6
90	71.8 ± 0.5	22.6 ± 0.2	5.6 ± 0.5	90	71.7 ± 0.5	22.8 ± 0.1	5.4 ± 0.5
120	70.8 ±0.4	23.3 ± 0.2	5.9 ± 0.4	120	71.0 ± 0.5	23.2 ± 0.2	5.8 ± 0.5
150	70.0 ±0.5	23.9 ± 0.3	6.1 ±0.4	150	69.7 ± 0.4	24.0 ± 0.2	6.3 ± 0.5
180	69.5 ± 0.2	24.5 ± 0.1	6.0 ±0.3	180	69.0 ± 0.6	24.1 ± 0.1	6.9 ± 0.7
210	68.6 ± 0.6	25.0 ± 0.3	6.5 ±0.7	210	68.3 ± 0.5	24.9 ± 0.2	6.7 ± 0.4

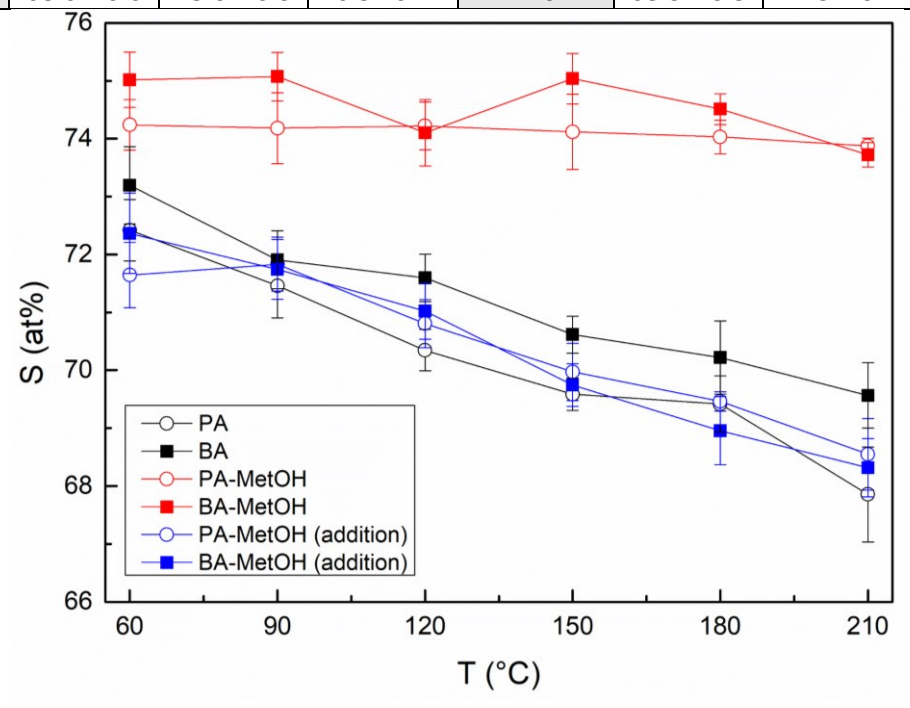


Figure 8: Annealing temperature dependence of sulfur content in $Ge_{20}Sb_5S_{75}$ thin films deposited from pure amines and mixtures of amine-methanol solvents.

The relative content of oxygen and nitrogen in deposited thin films is depicted in figure 9. Oxygen traces in thin films deposited from pure amines can be explained by minor oxidation during their transport in the ambient atmosphere to the FE-SEM/EDS chamber. However, there is a remarkable difference in oxygen content between thin films deposited from solutions of aminemethanol mixtures and solutions, where the methanol was added after glass dissolution. This confirms that methanol is clearly more firmly fixated in the matrix of thin films deposited from amine-methanol mixtures either due to significant structural differences of glass solutions, and probably also due to the lower films' porosity. With the increasing annealing temperature, the oxygen content decreases, regardless of the used amine, down to the oxygen level of thin films based on pure amines without methanol presence.

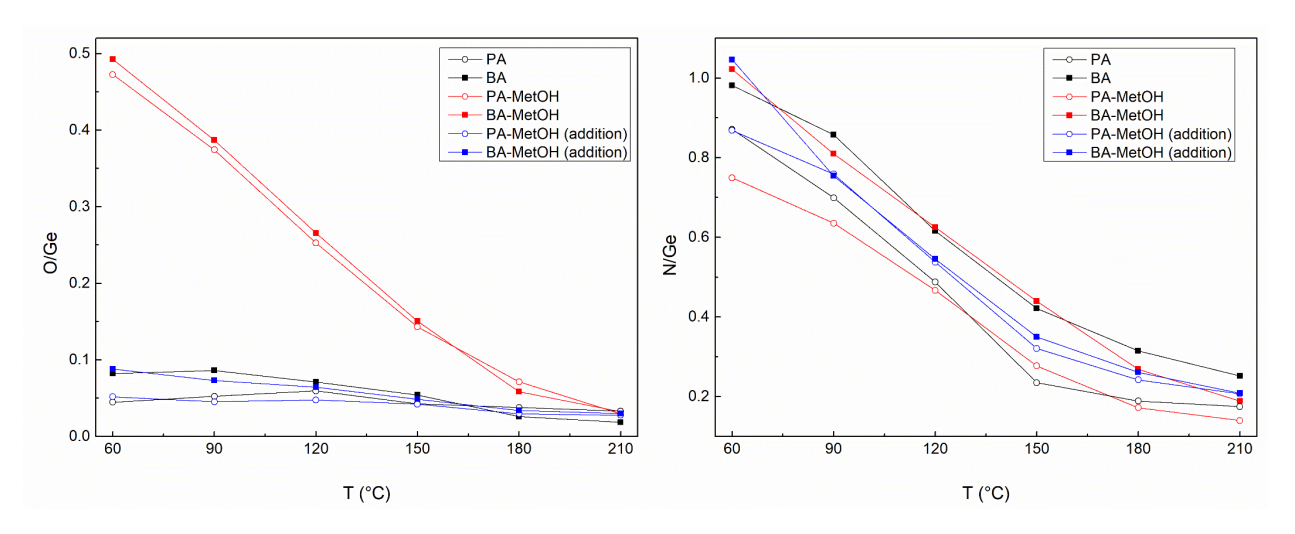


Figure 9: Annealing temperature dependences of relative oxygen (left) and nitrogen (right) content in spin-coated $Ge_{20}Sb_5S_{75}$ thin films deposited from pure amines and mixtures of amine-methanol solvents.

The nitrogen content represents the content of organic residuals from amine solvent and amine-glass reaction products. The nitrogen content steadily decreases with increasing annealing temperature. Measured data shows that nitrogen content is not affected by the presence of the methanol, but only shows minor differences based on the used amine. Thus, the methanol addition positively influences the composition of studied thin films while its presence does not hinder the critical step of organic residual removal.

Thermal dependence of thickness and relative thickness (Figure 10) of deposited $Ge_{20}Sb_5S_{75}$ thin films shows high thin film contractions, caused by massive removal of solvent residua and structural changes connected with glass polymerization. Measured spectra also demonstrated that all studied thin films possess specular optical quality (Figure S5 in supplementary materials). The data confirms earlier observations on solution-processed amorphous Ge-based thin films [30, 35], where a steep decrease in thickness occurs up to approximately 150°C and then it is followed more gradual decrease at higher annealing temperatures. However, the data also illustrates a significant difference between thin film deposited from pure amines and amine-methanol mixtures. Thin films prepared using amine-methanol mixtures exhibit film contraction by approximately 7.5% lower in comparison to the other studied thin films. The origin of the observed difference in thickness contraction could be credited to the higher sulfur release and higher porosity of the films deposited from pure amine solutions and solutions with methanol added after complete glass dissolution.

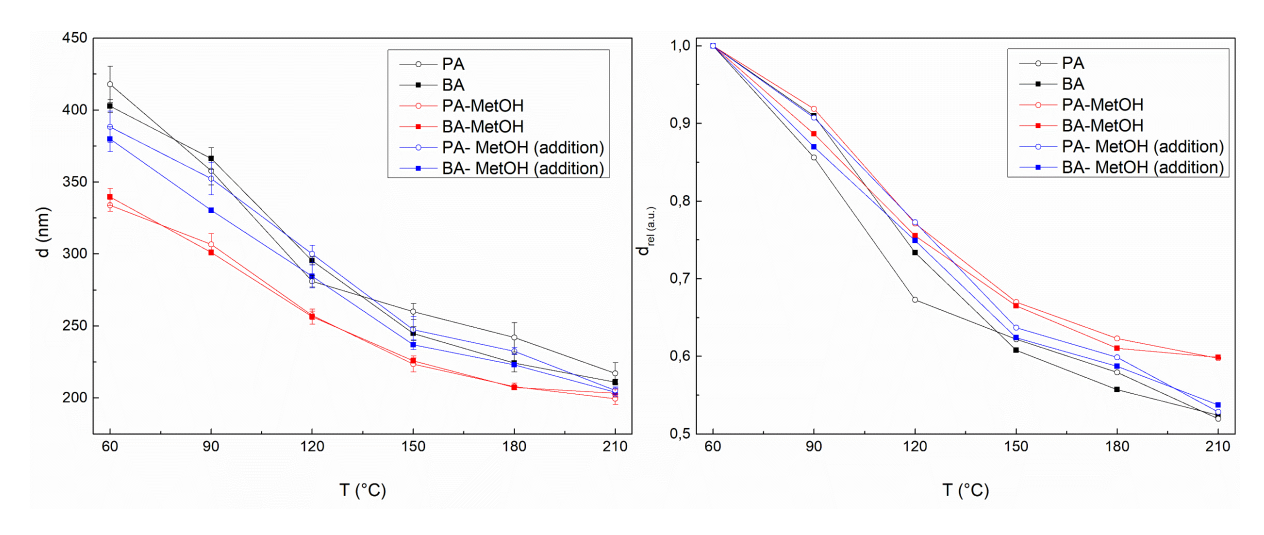


Figure 10: Annealing temperature dependences of thickness (left) and relative thickness (right) of spin-coated $Ge_{20}Sb_5S_{75}$ thin deposited from pure amines and mixtures of amine-methanol solvents.

The high optical quality of the prepared thin films was also confirmed by FE-SEM images (Figure S4), which do not show any surface microstructure or surface roughness. The low surface roughness was simultaneously confirmed by AFM measurements. Even the highest observed roughness RMS values of 1.30 (for the thin films deposited from the BA-MetOH mixture and annealed at 210 °C) could not affect their optical quality. AFM scans also show the presence of nanopores. Their occurrence has already been observed and previously described on As-S thin films deposited from similar solution [63]. The explanation for the formation of pores is a rapid evaporation of the used solvent from the volume of the thin film during the spin-coating stage of preparation. AFM scans show a higher amount of these pores in the thin films deposited from the amine-methanol mixtures, which is probably caused by the additional evaporation of a large amount of MetOH from the thin films during stabilization and annealing. This also corresponds to the EDS observation of the relative oxygen content in the thin films (Fig. 9 left).

We can speculate that thin films deposited from amine-methanol mixtures can also possess higher density connected with lower porosity. This proposition can be supported by their higher refractive index values in comparison with thin films deposited from solutions without methanol assistance during glass dissolution (Figure 11) [64 - 65]. As the annealing temperature increases, the structure of studied thin films changes, organic residuals are released and the refractive index rises. The EDS data showed that the thin films deposited from amine-methanol mixtures contain practically the same amount of amine residuals as other studied samples. At the same time, they simultaneously also contain a higher amount of methanol residuals and a higher content of sulfur (as low refractive index material). These facts alone would suggest that their refractive index should eventually be even lower than in the case of thin films deposited from solutions without methanol assistance during glass dissolution. Thus we assume that higher compactness (or lower porosity) is positively contributes to the higher refractive index of thin films deposited from amine-methanol solutions. It is also another significant advantage of such a multi-component solvent approach, which supports its potential usage in solution processing of other Ge-based systems.

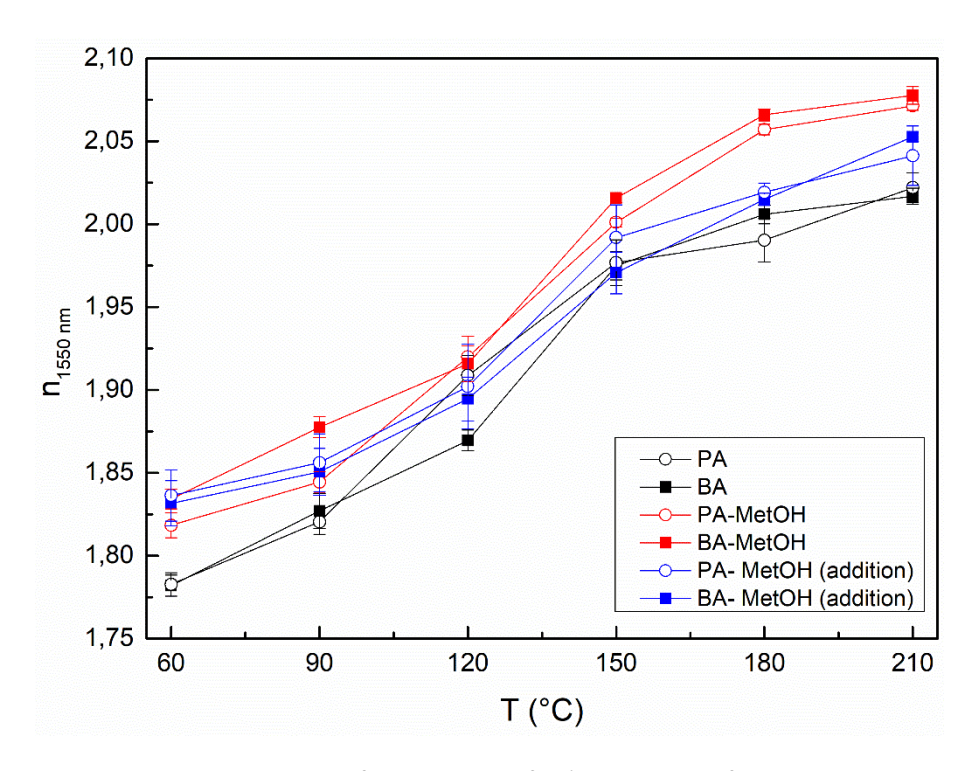


Figure 11: Annealing temperature refractive index for λ =1550 nm of spin-coated Ge₂₀Sb₅S₇₅ thin deposited from pure amines and mixtures of amine-methanol solvents.

Conclusions

The $Ge_{20}Sb_5S_{75}$ chalcogenide glass was successfully dissolved and spin-coated from pure n-propylamine, n-butylamine, and their mixtures with 10% methanol. The solutions with the presence of methanol were significantly darker and their Raman spectra were notably different from their pure amine counterparts. The Raman spectra of glass solutions prepared from amine-methanol mixtures confirmed higher structural fragmentation caused by further splitting of the $Ge_4S_{10}^{4-}$ cluster structure. The addition of methanol after complete glass dissolution resulted in only partial changes in the structure, which were attributed to changes in post-dissolution equilibrium. However, the simple addition of methanol into the already prepared solution did not result in the same glass fragments. The Raman spectra of pure dissolved sulfur and antimony-free $Ge_{25}S_{75}$ chalcogenide glass proved that the observed decline of $Ge_4S_{10}^{4-}$ bands in solutions based on amine-methanol mixtures is connected directly to both the methanol and antimony presence.

Different dissolving mechanisms of $Ge_{20}Sb_5S_{75}$ in pure amines and mixtures of pure amines with methanol significantly impacted the properties of prepared thin films. The structure of as-prepared thin films deposited from pure amine glass solutions consisted of highly fragmented corner-shared $GeS_{4/2}$ tetrahedrons structure formed from $Ge_4S_{10}^{4-}$ compounds present in the source solution. On the contrary, the structure of as-prepared thin films deposited from amine-methanol mixtures was more polymerized. It consisted of both the corner- and edge-shared $GeS_{4/2}$ tetrahedrons with a high content of non-bonded sulfur in the form of the S_8 rings probably due to the rapid re-polymerization of the highly fragmented structural units during the thin film formation and solidification. With increasing annealing temperature, the structure of studied thin films shifts towards the structure of the original bulk glass. However, thin films prepared from a solution of glass dissolved in aminemethanol mixtures proved significantly higher compositional stability, lower thickness contraction, and slightly higher refraction index in comparison to the glass dissolved in pure amines without the costs

of the lower ability for organic residuals removal. These facts make the multi-component aminemethanol solvent approach highly advantageous and substantially better than pure amines.

Thus, the methanol presence in the source amine solution significantly alters the Ge-Sb-S dissolution mechanism. It leads not only to different ratio of structural units present in the prepared solution, but also positively affects the properties of deposited thin films. They possess a higher refractive index, undergo lower thermally-induced surface contraction, and maintain the stable elemental composition in comparison with thin films deposited from traditional pure amine solvents.

Acknowledgements

Authors appreciate the financial support from projects "High-sensitive and low-density materials based on polymeric nanocomposites" − NANOMAT (№ CZ.02.1.01/0.0/0.0/17_048/0007376) from European Regional Development Fund, grant LM2023037 from the Ministry of Education, Youth and Sports of the Czech Republic and project OISE-2106457 from NSF Ires1 program.

References

- [1] B.J. Eggleton, B. Luther-Davis and K. Richardson, Nat. Photon., **5**, (2011) 141-148. https://doi.org/10.1038/nphoton.2011.309
- [2] G.E. Snopatin, V.S. Shiryaev, B.G. Plotnichenko, E.M. Dianov and M.F. Churbanov, Inorg. Mater., 45 (2009) 1439-1460. https://doi.org/10.1134/S0020168509130019
- [3] S. Li, X. Li, Z. Ren and Q. Zhang, J. Mater. Chem. A, 6, (2018) 2432-2448. https://doi.org/10.1039/C7TA09941J
- [4] J.L. Adam and X. Zhang, Chalcogenide Glasses: Preparation, Properties and Applications, Woodhead Publishing Limited (2014).
- [5] Ch. Chang and H. Tuan, Chem. Asian J., 17 (2022) e202200170. https://doi.org/10.1002/asia.202200170
- [6] R. Singh, P. Kumar, T. Ichikawa and A. Jain, Molecules, 25 (2020) 3733. https://doi.org/10.3390/molecules25163733
- [7] M. Xu, X. Mai, J. Lin, W. Zhang, Y. li, Y. He, H. Tong, X. Hou, P. Zhou and X. Miao, Adv. Funct. Mater., 30 (2020) 2003419. https://doi.org/10.1002/adfm.202003419
- [8] A.S. Hassanien, I. Sharma and K.A. Aly, Physica B Condens, 613(2021) 412985. https://doi.org/10.1016/j.physb.2021.412985
- [9] I. Csarnovics, M.R. Latif, T. Nichol, W. Kuang, M. Mitkova, M. Veres and S. Kokenyesi, Mater. Sci. Eng. A, 5 (2015) 78-86. https://doi.org/10.17265/2161-6213/2015.1-2.011
- [10] Y. Saito, M. Morota, K. Makino, J. Tominaga, A.V. Kolobov and P. Fons, Mater. Sci. Semicond. Process, 135 (2021) 106079. https://doi.org/10.1016/j.mssp.2021.106079
- [11] S. Mormani, G. Louvet, E. Baudet, M. Bouska, J. Gutwirth, F. Starecki, J.L. Doualan, Y. Ledemi, Y. Messaddeq, J.L. Adam, P. Nemec and V. Nazabal, Sci. Rep., 10 (2020) 7997. https://doi.org/10.1038/s41598-020-64092-3
- [12] L. Mochalov, A. Nezhdanov, D. Usanov, A. Markelov, V. Trushin, G. Chidichimo, G. De Filpo,
 D. Godova and A. Mashin, Superlattices Microstruct.,111 (2017) 173-180.
 https://doi.org/10.1016/j.spmi.2017.06.030
- [13] S. Song, N. Carlie, J. Boudies, L. Petit, K. Richardson and C.B. Arnold, J. Non-Cryst. Solids, 355(2009) 2272-2278. https://doi.org/10.1016/j.jnoncrysol.2009.07.015
- [14] Y. Zou, H. Lin, O. Ogbuu, L. Li, S. Danto, S. Novak, J. Novak, J.D. Musgraves, K. Richardson and J. Hu, Opt. Mater. Express, 2 (2012) 1723-1732. https://doi.org/10.1364/OME.2.001723
- [15] S. Novak, P.T. Lin, Ch. Li, Ch. Lumdee, J. Hu, A. Agarwal, P.G. Kik, W. Deng and K. Richardson, ACS Appl Mater Interfaces, 9 (2017) 26990–26995. https://doi.org/10.1021/acsami.7b06140

- [16] S. Novak, D.E. Johnson, Ch. Li, W. Deng and K. Richardson, Thin Solid Films, 588 (2015) 56-60. https://doi.org/10.1016/j.tsf.2015.04.049
- [17] E.A. Sanchez, M. Waldmann and C.B. Arnold, Appl. Optics, 50 (2011) 1974-1978. https://doi.org/10.1364/AO.50.001974
- [18] B.S. Yadav, S.R. Dey and S.R. Dhage, Appl. Surf. Sci. Adv., 6 (2021) 100144. https://doi.org/10.1016/j.apsadv.2021.100144
- [19] S. Chand, N. Thakur, S.C. Katyakm P.B. Barman, V. Sharma and P. Sharma, Sol. Energy Mater. Cells, 168 (2017) 183-200. https://doi.org/10.1016/j.solmat.2017.04.033
- [20] U. Chalapathi, B. Poornaprakash, C-H. Ahn and S-H. Park, Appl. Surf. Sci., 451 (2018) 272-279. https://doi.org/10.1016/j.apsusc.2018.04.249
- [21] Ch. Li, S. Novak, S.A. Denisov, N.D. McClenaghan, N. Patel, A. Agarwal, K. Richardson and W. Deng, Thin Solid Films, 626 (2017), 194-199. https://doi.org/10.1016/j.tsf.2017.02.030
- [22] Ch. Lu, M.P. Almeida, N. Yao and C. Arnold, Appl. Phys. Lett., 105 (2014) 261906. https://doi.org/10.1063/1.4905283
- [23] S. Novak, L. Scarpantonio, J. Novak, M.D. Pre, A. Martucci, J.D. Musgraves, N.D. McClenaghan and K. Richardson, Opt. Mater. Express, 3 (2013) 729-738. https://doi.org/10.1364/OME.3.000729
- [24] S. Slang, L. Loghina, K. Palka and M. Vlcek, RSC Adv., 7 (2017) 53830-53838. https://doi.org/10.1039/c7ra09540f
- [25] K. Palka, S. Slang, J. Buzek and M. Vlcek, J. Non-Cryst. Solids, 447 (2016) 104-109. https://doi.org/10.1016/j.jnoncrysol.2016.05.042
- [26] P. Sachan, R. Singh, P.K. Dwivedi and A. Sharma, RSC Adv., 8 (2018) 27946-27955. https://doi.org/HYPERLINK "https://doi.org/10.1039/C8RA03249A"10.1039/C8RA03249A
- [27] S. Tsadka, N. Ostrovsky, E. Toledo, G. Le Saux, E. Kassis, S. Joseph and M. Schwartzman, Opt. Express, 19 (2020) 28352-38365. https://doi.org/10.1364/OE.400038
- [28] S. Slang, P. Janicek, K. Palka, L. Loghina and M. Vlcek, Mater. Chem. Phys., 203 (2018) 310-318. https://doi.org/10.1016/j.matchemphys.2017.10.025
- [29] G.C. Chern and I. Lauks, J. Appl. Phys., 53 (1982) 6979-6982. https://doi.org/10.1063/1.330043
- [30] S. Slang, P. Janicek, K. Palka and M. Vlcek, Opt. Mater. Express,6 (2016) 1973-1985. https://doi.org/10.1364/OME.6.001973
- [31] J. Novak, S. Novak, M. Dussauze, E. Fargin, F. Adamietz, J.D. Musgraves and K. Richardson, Mater. Res. Bull., 48 (2013) 1250-1255. https://doi.org/10.1016/j.materresbull.2012.12.008
- [32] H. Khan, M. Husain and M. Zulfewuar, Results in Optics, 11 (2023) 100412. https://doi.org/10.1016/j.rio.2023.100412
- [33] Ch.Li, S. Novak, S.A. Denisov, N.D. McClenaghan, N. Patel, A. Agarwal, K. Richardson and W. Deng, Thin Solid Films, 626 (2017) 194-199. https://doi.org/10.1016/j.tsf.2017.02.030
- [34] S. Novak, P.T. Lin, Ch. Li, N. Borodinov, Z. Han, C. Monmeyran, N. Patel, Q. Du, M. Malinowski, S. Fathpour, Ch. Lumdee, Ch. Xu, P.G. Kik, W. Deng, J. Hu, A. Agarwal, I. Luzinov, K. Richardson, J. Vis. Exp., 114 (2016) 54379. https://doi.org/10.3791/54379
- [35] S. Slang, K. Palka, J. Jancalek, M. Kurka and M. Vlcek, Opt. Mater. Express, 10 (2020) 2973-2986. https://doi.org/10.1364/OME.408327
- [36] K. Schmidt, L. Bauch, G. Kluge and P. Süptitz, Phys. Status Solidi, 113 (1989) 55-59.
- [37] H. Khan, P.K. Dwivedi, S. Islam, M. Husain and M. Zulfequar, Opt. Mater., 119 (2021) 111332. https://doi.org/10.1016/j.optmat.2021.111332
- [38] M. Waldmann. J.D. Musgraves, K. Richardson and C.B. Arnold, J. Mater. Chem., 22 (2012) 17848-17852. https://doi.org/10.1039/C2JM32235H
- [39] M. Wachhold, K.K. Rangan, M. Lei, M.F. Thorpe, S.J.L. Billinge, V. Petkov, J. Heising and M.G. Kanatzidis, J. Solid State Chem., 152 (2000) 21-36. https://doi.org/10.1006/jssc.2000.8673

- [40] M.J. MacLachlan, N. Coombs, and G.A. Ozin, Nature, 397 (1999) 681–684. https://doi.org/10.1038/17776
- [41] M.J. MacLachlan, S. Petrov, R.L. Bedard, I. Manners and G.A. Ozin, Angew. Chem. Int. Ed.,37 (1998) 2076-2079. <a href="https://doi.org/10.1002/(SICI)1521-3773(19980817)37:15<2075::AID-ANIE2075>3.0.CO;2-L">https://doi.org/10.1002/(SICI)1521-3773(19980817)37:15<2075::AID-ANIE2075>3.0.CO;2-L
- [42] K.K. Rangan, P.N. Trikalitis and M.G. Kanatzidis, J. Am. Chem. Soc., 122 (2000) 10230-10231. https://doi.org/10.1021/ja002362c
- [43] S. Slang, P. Janicek, K. Palka and M. Vlcek, Opt. Mater. Express, 9 (2019) 4360-6369. https://doi.org/10.1364/OME.9.004360
- [44] R. Swanepoel, J. Phys. Sci. Instrum., 16 (1983) 1214-1222. https://doi.org/10.1088/0022-3735/16/12/023
- [45] S.H. Wemple and M. Didomenico, Phys. Rev. B., 3 (1971) 1338-1351. https://doi.org/10.1103/PhysRevB.3.1338
- [46] B. Yang, D.J. Xue, M. Leng, J. Zhong, L. Wang, H. Song, Y. Zhou and J. Tang, Sci. Rep., 5 (2015) 10978. https://doi.org/10.1038/srep10978
- [47] K.K. Kalebaila, D.G. Georgiev and S.L. Brock, J. Non-Cryst. Solids, 352 (2006) 232-240. https://doi.org/10.1016/j.jnoncrysol.2005.11.035
- [48] M. Yamaguchi, T. Shibata and K. Tanaka, J. Non-Cryst. Solids, 232-234 (1998) 715-720. https://doi.org/10.1016/S0022-3093(98)00439-6
- [49] J.T. Sutherland, S.A. Poling, R.C. Belin and S.W. Martin, Chem. Mater., 16 (2004) 1226-1231. https://doi.org/10.1021/cm034990+
- [50] A. Chrissanthopoulos, P. Jovari, I. Kaban, S. Gruner, T. Kavetskyy, J. Borc, W. Wang, J. Ren, G. Chen and S.N. Yannopoulos, J. Solid State Chem., 192 (2012) 7-15. https://doi.org/10.1016/j.jssc.2012.03.046
- [51] Z. Li, K. Wang, J. Zhang, F. Chen, Ch. Lin, S. Dai and W. Ji, J. Non-Cryst. Solids, 588 (2022) 121628. https://doi.org/10.1016/j.jnoncrysol.2022.121628
- [52] S.A. Poling, C.R. Nelson, J.T. Sutherland and S.W. Martin, J. Phys. Chem. B, 107 (2003) 5413-5418. https://doi.org/10.1021/jp027313w
- [53] F.P. Daly and C.W. Brown, J. Phys. Chem., 77 (1973) 1859-1861.
- [54] F.P. Daly and C.W. Brown, J. Phys. Chem., 79 (1975) 350-354.
- [55] R. Golovchak, V. Nazabal, B. Bureau, J. Oelgoetz, A. Kovalskiy and H. Jain, J. Non-Cryst. Solids, 499 (2018) 237-244. https://doi.org/10.1016/j.jnoncrysol.2018.07.040
- [56] C.R. Nelson, S.A. Poling and S.W. Martin, J. Non-Cryst. Solids, 337 (2004) 78-85. https://doi.org/10.1016/j.jnoncrysol.2004.03.103
- [57] T. Haizheng, Z. Xiujian and J. Chengbin, J. Mol. Struct., 697 (2004) 23-27. https://doi.org/10.1016/j.molstruc.2003.12.039
- [58] Ch. Lin, Z. Li, L. Ying, Y. Xu, P. Zhang, S. Dai, T. Xu and Q. Nie, J. Phys. Chem. C, 116 (2012) 5862-5867. https://doi.org/10.1021/jp208614j
- [59] G.C. Chern, I. Lauks and A.R. McGhie, J. Appl. Phys., 54 (1983) 4596-4601. https://doi.org/10.1063/1.332614
- [60] S. Song, J. Dua and C.B. Arnold, Opt. Express, 18 (2010) 5472-5480. https://doi.org/10.1364/OE.18.005472
- [61] GESTIS Substance Database, https://gestis-database.dguv.de/data?name=038390, (accessed May 2023).
- [62] GESTIS Substance Database, https://gestis-database.dguv.de/data?name=010750, (accessed May 2023).
- [63] Y. Zha, S. Fingerman, S.J. Cantrell and C.B. Arnold, J. Non-Cryst. Solids, 369 (2013) 11-16. http://dx.doi.org/10.1016/j.jnoncrysol.2013.03.014
- [64] A. Perrotta, P. Poodt, F.J. van den Bruele, W.M.M. Kessels and M. Creatore, Dalton. Trans., 47 (2018) 7649-7655., https://doi.org/10.1039/C8DT01246F
- [65] A.S. Hassanien, I. Sharma and A.A. Akl, J. Non-Cryst. Solids, 531 (2020) 119853. https://doi.org/10.1016/j.jnoncrysol.2019.119853